

Article

Structure-Based Modeling of the Mechanical Behavior of Cross-Linked Enzyme Crystals

Marta Kubiak *, Ingo Kampen and Carsten Schilde

Institute for Particle Technology, Technische Universität Braunschweig, Volkmaroder Str. 5, 38104 Braunschweig, Germany; i.kampen@tu-bs.de (I.K.); c.schilde@tu-bs.de (C.S.)

* Correspondence: marta.kubiak@tu-braunschweig.de; Tel.: +49-(0)53139165533

Abstract: Because of their high volumetric catalytic activity, in addition to their high chemical and thermal resistances, enzymes in the form of protein crystals are an excellent choice for application as immobilized biocatalysts. However, mechanical stability is a requirement for the processability of immobilisates, in addition to the protein crystals retaining their enzymatic activity, and this is closely related to the crystal structure. In this study, the influence of protein engineering on the mechanical stability of cross-linked enzyme crystals (CLECs) was investigated using a genetically modified model protein in which additionally cysteines were introduced on the protein surface for targeted cross-linking. The results showed that the mechanical stability of crystals of the mutant proteins in the native form was decreased compared to native wild-type crystals. However, specific cross-linking of the introduced amino acid residues in the mutant proteins resulted in their increased mechanical stability compared to wild-type CLECs. In order to determine the correlation between the crystal structure and the resulting mechanical properties of CLECs to enable targeted cross-linking, a previously developed model was revised and then used for the two model proteins. This model can explain the mechanically investigated relationships, such as the anisotropic crystal behavior and the influence of a linker or mutation on the micromechanical properties and, hence, can be helpful for the tailor-made production of CLECs.



Citation: Kubiak, M.; Kampen, I.; Schilde, C. Structure-Based Modeling of the Mechanical Behavior of Cross-Linked Enzyme Crystals. *Crystals* **2022**, *12*, 441. <https://doi.org/10.3390/cryst12040441>

Academic Editor: Abel Moreno

Received: 1 March 2022

Accepted: 19 March 2022

Published: 22 March 2022

Publisher's Note: MDPI stays neutral with regard to jurisdictional claims in published maps and institutional affiliations.



Copyright: © 2022 by the authors. Licensee MDPI, Basel, Switzerland. This article is an open access article distributed under the terms and conditions of the Creative Commons Attribution (CC BY) license (<https://creativecommons.org/licenses/by/4.0/>).

Keywords: protein engineering; CLECs; modeling

1. Introduction

In comparison to chemical synthesis, enzyme-catalyzed reactions proceed with high chemo-, regio-, and enantioselectivity [1,2]. Because of their high efficiency, environmental friendliness, and safety [3,4], they are widely used in numerous industrial sectors, such as pharmaceutical research, food modification, biofuel development, agroindustry, and laundry [5]. The great application potential of enzymes has led to huge growth in their consumption, which is why the global market for enzymes was estimated at \$9.9 billion in 2019 and is expected to grow with an annual average growth rate of 7.1% from 2020 to 2027 [6].

However, the advantages are offset by the high requirements of the enzymes with regard to the very defined and mild reaction conditions, such as temperature, pressure, or solvents used [7,8]. Their technical use is also limited by low long-term stability, as well as difficult processability and reusability [9]. Therefore, to ensure the efficient application of enzymes in biocatalysis, some optimization in terms of stability, activity, or tolerance to the solvents is necessary [10]. Originally, in order to increase the efficiency of the biocatalysts, the reaction conditions of synthesis were adapted to the enzyme requirements, leading to the development of the so-called medium engineering approach [11–13]. In the meantime, the focus is shifting to the development of other strategies for improving the performance of biocatalysts. Two possible concepts that can effectively contribute to the improvement of enzyme properties are protein engineering and enzyme immobilization. Protein engineering aims to improve enzyme properties, such as activity or selectivity, through selective

manipulation of amino acids. In immobilization, a soluble enzyme is physically separated or localized in a confined space while retaining its catalytic activity [14]. This can result in an increase in productivity and enzyme lifetimes, as well as improvement in handling and facilitation of recovery [15]. The simultaneous use of both strategies led to the emergence of a new field of research called immobilized biocatalyst engineering in which the aim is to produce tailor-made immobilized biocatalysts for use in bioprocesses [16]. One of the most convincing concepts for the stabilization and immobilization of enzymes is to cross-link enzymes in their crystalline state. Such cross-linked enzyme crystals (CLECs) remain active under comparatively extreme conditions of temperature, pH, or organic solvent content [17]. In addition, CLECs show high resistance against autolysis and degradation by proteases and show good storage stability at room temperatures [18].

However, the production of efficient, tailor-made CLECs is limited by the lack of understanding of the relationship between an enzyme's structure and the resulting properties of the crystals built from that enzyme. In addition to the enzyme itself, the mechanical stability of these protein crystals is closely related to the crystal structure. The challenge of protein engineering lies in the prediction of potential amino acid sequence changes in order to obtain suitable protein structures that then fulfill the specified functions. Due to the complex and individual behavior of enzymes, it is extremely difficult to predict the overall effect of a sequence change on the structure and, thus, on the function. To be able to produce tailor-made CLECs, all the interactions, limitations, and influences along the entire production chain, starting from the sequence to the product, must therefore be investigated and elucidated.

In this study, the influence of protein engineering on the mechanical stability of CLECs was investigated and modeled based on a model protein, namely, halohydrin dehalogenase (HheG), which is used, for example, to remove haloalcohols in food applications [19]. As a basis, amino acids on the surface of the folded wild-type enzyme structure were genetically exchanged using protein engineering methods, as described in Staar et al. [17], to incorporate new potential cross-linking sites within the subsequently fabricated protein crystals and thus improve the mechanical crystal properties. The focus was on elucidating the structure–property and sequence–property relationships based on the performed experiments. For this purpose, a previously developed model [20] was expanded and then validated using the new crystals presented here, as well as for various cross-linked wild-type crystals. The results of our study establish the fundamentals for the desired formulation of reinforced catalytic active crystalline biocatalysts and, therefore, their expanded applications in industrial processes.

2. Materials and Methods

2.1. Experimental Procedure

In order to reliably measure the mechanical properties, certain requirements with regard to crystallization must be met: The crystals must (i) adhere to the surface of the sample holder, (ii) be present in individual units, (iii) the crystal shape must be fully formed, and (iv) the crystal face should be placed orthogonal to the direction of measurement. Furthermore, crystals must (v) have a minimum particle size (approximately 70 μm) and (vi) exhibit reproducible production. Analogous to crystallization, the subsequent cross-linking also had to meet certain criteria, such as (i) complete and homogeneous cross-linking within the crystal, (ii) no negative influence on the catalytic activity, (iii) no change in the surface properties of the crystals, (iv) no crystal damage after cross-linking, and (v) no detachment of the crystals from the surface of the sample carrier. Figure 1 shows a sample of cross-linked HheG crystals that completely fulfills these requirements.

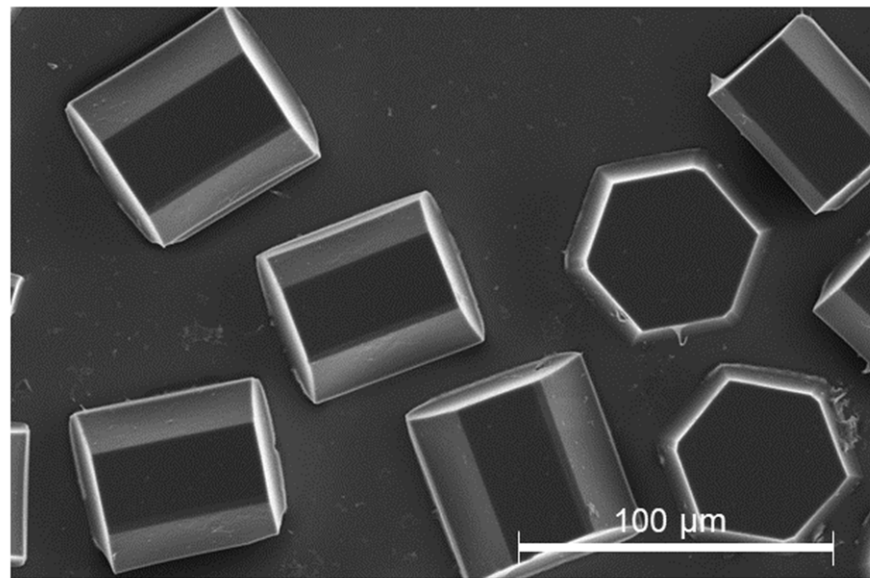


Figure 1. Cross-linked hexagonal HheG wild-type crystals.

In order to examine the structure–property relationships of CLECs, the model protein halohydrin dehalogenase HheG from *Ilumatobacter coccineus* (HheG) was produced and purified by the working group of Prof. A. Schallmey from the Institute for Biochemistry in Braunschweig and provided for the experimental study. In addition, through mutagenesis of the wild-type HheG proteins, aspartic acid was exchanged for cysteine at position 114 to insert a new cross-linking site for BMOE (bismaleimidoethane) on the surface of the protein, as previously described [17].

An AFM (Bruker NanoWizard3, former JPK) and a classical nanoindenter (Hysitron TriboIndenter Ti900) were used to characterize the mechanical properties at different scales. The AFM allowed for the mechanical properties of the surface at low forces to be investigated by generating small penetration depths in the nanometer range (compare with [20,21]). The nanoindenter allowed for the use of much higher indentation forces such that mechanical behavior at large penetration depths can be investigated. The mechanical investigation at both depth ranges was of particular interest from a modeling view, which was based on a molecular crystal structure. With just a few molecules, the number of data points that needed to be processed was already in the seven-digit range. This posed a major computational problem due to the limitations of computational capacity. Hence, the modeling had to be limited to a relatively small crystal section. To verify whether the model reproduced the mechanical properties within the entire crystal, depth-dependent mechanical measurements were performed using an AFM and a nanoindenter.

2.2. Crystallization and Cross-Linking

Wild-type halohydrin dehalogenase HheG and mutated HheG proteins (D114C) were crystallized using a sitting drop method such that the crystals were grown on a siliconized slide and, hence, they adhered to the surface (compare Section 2.1). A 20 μ L droplet composed of protein stock solution (32 mg/mL for wild-type HheG and 24 mg/mL for D114C) and precipitation solution (PEG 4000 (10% (*w/v*) in HEPES buffer (10 mM, pH 7.3)) was placed on a cover slide and equilibrated against reservoir solution (500 μ L) at 5 $^{\circ}$ C for a few days.

The procedure for cross-linking followed already established rules [20]. First, the mother liquor was removed to get rid of any remaining free proteins in the droplet, which would otherwise also be cross-linked and form an undefined precipitate. For this purpose, the sample with the crystals had to be placed on ice for about one hour to reduce the osmotic shock during the solution change and avoid crystal breakage [22]. The crystals

were subsequently washed several times by adding about 10 μ L of the crystallization solution to the crystals and carefully wiping it off with precision wipes without touching the crystals. Depending on the cross-linking method, the linker was added either directly onto the crystals (soaking method) or into a reservoir so that the crystals were cross-linked via the vapor diffusion and hanging drop method. Five cross-linkers having different lengths and properties, as shown in Table 1, were applied for the cross-linking of the model protein crystals.

Glutaraldehyde solution 50% (Sigma-Aldrich Chemie GmbH, Taufkirchen, Germany) is the most commonly used linker for cross-linking protein crystals. DMP (dimethyl pimelidate), DST (disuccinimidyl tartrate), and Sulfo-EGS (ethylene glycol bis(sulfosuccinimidyl succinate)), purchased from Thermo Fisher Scientific, are specific lysine linkers with a well-defined length. These linkers were used for cross-linking wild-type HheG crystals. BMOE purchased from Thermo Fisher Scientific is a cysteine linker and was applied for the D114C crystals, where a cysteine residue was introduced by protein engineering.

Table 1. Length and conjugation of the used linkers.

Cross-Linker	Length (Å)	Conjugation
Glutaraldehyde (GA)	~5 and longer	Amines (lysine, arginine)
DMP	~9	Amines (lysine)
DST	~6	Amines (lysine)
Sulfo-EGS	~16	Amines (lysine)
BMOE	~8	Sulfhydryls (cysteine)

For the AFM-based nanoindentation, the wild-type HheG crystals were cross-linked using a soaking method with either a glutaraldehyde solution (5% (*v/v*)) or a mix of three different linkers (DMP, DST, and Sulfo-EGS), according to Table 2. For the mechanical investigation using a nanoindenter, both the wild-type and D114C HheG crystals were cross-linked with glutaraldehyde using a vapor diffusion method (25% (*v/v*)), as previously described [22]. After that, some of the samples of the D114C crystals were additionally cross-linked using a soaking method and the BMOE cross-linker. For mechanical quantification of cysteine cross-linking, a BMOE single cross-linker was also used for the cross-linking of D114C crystals. Table 2 summarizes the cross-linking conditions. According to Kubiak et al., 24 h is needed for complete cross-linking of HheG crystals. For that reason, all the samples were always cross-linked over 24 h.

Table 2. Stock solutions for the cross-linking. The solutions of BMOE and DST were diluted with a mixture of TE and HEPES buffer to a final concentration of 2 and 4 mM, respectively.

	Glutaraldehyde	BMOE	DST	DMP	Sulfo-EGS
Concentration	5% or 25%	20 mM	40 mM	4 mM	4 mM
Solvent	HEPES buffer	DMSO	DMSO	TE and HEPES buffer	

2.3. Mechanical Measurements

Methods for mechanical characterization of protein crystals were already established and are described in detail in previous publications for AFM-based nanoindentation [20,21,23] and classical nanoindentation using a nanoindenter [22]. As previously reported, CLECs were mechanically investigated in a liquid environment. For the AFM measurements, a spherical cantilever with a radius of 150 nm and a nominal spring constant of 40 N/m was used. The nanoindentation was performed with a Berkovich tip at 5 °C in a displacement-controlled mode. Further information about, e.g., detailed measurement parameters, can be found in the publications of Kubiak et al. [20,21,23].

2.4. Modeling of Anisotropic Crystal Strength

Based on the crystal structure, a structural model was developed to represent the mechanical behavior of cross-linked crystals at the structural level. MATLAB version R2017a software was used for this purpose. The procedure for modeling the mechanical behavior of the crystals was described in detail in the publication of Kubiak et al. [20] and is repeated with permission in this publication. The developed toolbox allows for reading the Protein Data Bank file format (.pdb), which represents the structure of three-dimensional molecules based on the atomic coordinates of amino acids of the protein. A .pdb file format contains coordinates from the smallest unit of the crystal (the so-called asymmetric unit), which can be multiplied to a larger crystal structure according to the given symmetry operators, which are also present in the file. The developed model allows for rebuilding the whole crystal using the symmetry operators, searching for atoms of relevant amino acids residues, e.g., sulfur atoms of the cysteine residues, and calculating the distances between them (cf. Figure 2). The amino acid residues that would be cross-linked by glutaraldehyde were determined based on the literature [24–27]. According to those studies, cross-linking bonds can be expected between three residual pairs: the ϵ -amines of lysine residues (Lys–Lys), two neighbored arginine residues (Arg–Arg), and arginine and lysine residues (Lys–Arg) having a maximal distance of 10 Å to each other (cf. [20]). For alternative cross-linkers (e.g., BMOE) the distance and the amino acids residues were adapted according to Table 1. For the crystals, all bonds within a unit cell and its surrounding of 100 Å (50 asymmetric units) were considered.

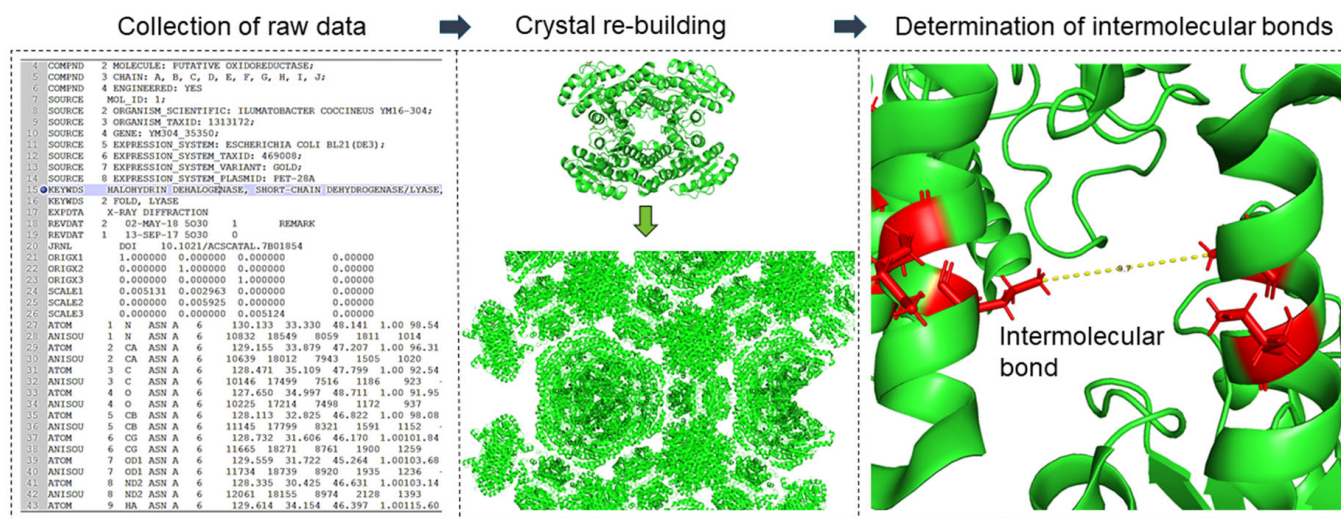


Figure 2. Overview approach to modeling mechanical crystal behavior based on crystal structure: investigation and classification of inter- and intramolecular cross-linking bonds.

Then, possible cross-linking bonds were analyzed regarding their distance and direction. Finally, the directions of the bonds in relation to the mechanically stressed crystal face were considered in order to calculate the direction-dependent crystal strength. For the investigation of the anisotropic crystal strength, the intra- and intermolecular bonds were considered separately, assuming that only the intermolecular bonds contribute to the improvement of the stability of the crystal structure in an environment other than the crystallization cocktail [20]. Furthermore, the strength of these bonds depends on their orientation with respect to the applied force during indentation, according to Figure 3.

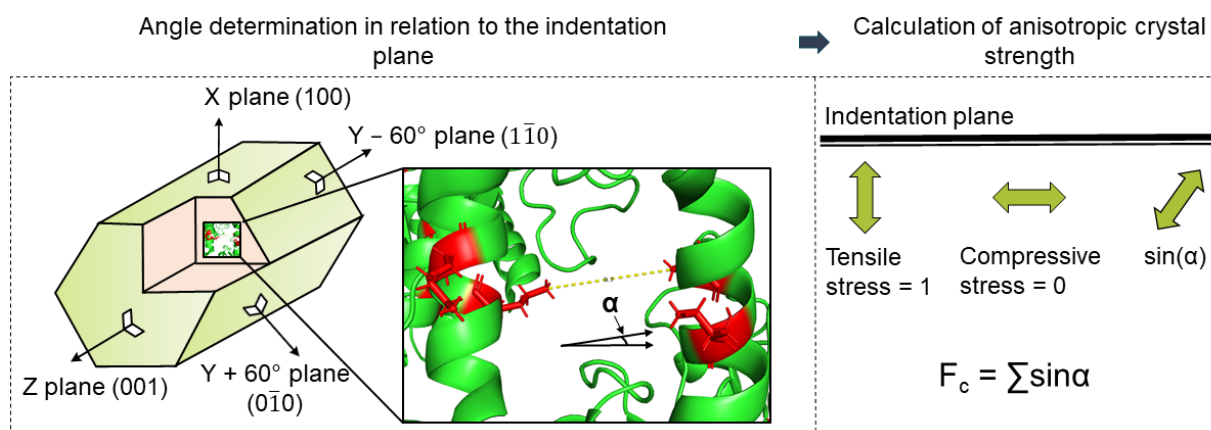


Figure 3. Overview approach to modeling mechanical crystal behavior based on crystal structure: calculation of anisotropic crystal strength using a direction of cross-linking bonds in relation to the indentation plane.

Similar studies on anisotropic particle strength as a function of porosity, particle structure, or size were published in the current literature [28–30]. Rumpf investigated a continuum-based model for determining the tensile strength of aggregates. It was based on assessing all partial stress contributions in a cross-sectional area of the structure in the direction of the applied force [28]. Schilde et al. reported that this model can also be applied to the compressive strength of aggregates measured via nanoindentation [29–31]. Based on these results, the fraction of each bond in the loading direction was calculated for each loaded crystal face. For this purpose, the sine of the angle between the normal of the crystal surface (\perp) and the direction of the bond was used as a factor. The determination of the directional crystal faces (the planes), which were used as the surface normal in the calculation, was achieved using the geometry data of the unit cell and the plane equations. As long as the function of bond strengths in terms of type and length was unknown, they were assumed to be equal and length-independent. Under this assumption, each bond was mapped to all the normal vectors of the crystal surface, as shown in Figure 3. In this way, a representative value for the total strength of the crystal surface was obtained. All the bonds were then summed proportionally to each face (resistance of the cross-linking bridges to the normal force).

3. Results and Discussion

3.1. Mechanical Properties of Wild-Type HheG Crystals in the Nanometer Range

Due to the increasing demands on the tailored properties of CLECs in terms of enzymatic activity, as well as mechanical stability, the elucidation of the relationships between the structure and the resulting properties is of particular interest. One of the most widely used linkers in the design of CLECs is glutaraldehyde [32–34]. However, according to the manufacturer's instructions, highly concentrated glutaraldehyde can be an irritant, toxic, or carcinogenic. In addition, reports indicate that excessive cross-linking with glutaraldehyde can lead to a reduction in catalytic activity [35]. For these reasons, the motivation to search for alternative cross-linkers increases. Previous studies have reported on the micromechanical properties of wild-type HheG CLECs [20], as well as the dominating influence of cross-linking bonds on the mechanical behavior of enzyme crystals [22]. The present study focused on modeling the properties of cross-linked enzyme crystals such that the selection of linkers and their influence on the mechanical and, if necessary, catalytic properties can be explained and predicted. Figure 4 compares the mechanical properties of wild-type crystals cross-linked with different linkers. Alternatively, for the glutaraldehyde, a mixture of three lysine linkers of defined length (6, 9, and 16 Å) was used for cross-linking. A single linker would not be sufficient to adequately cross-link the crystals; therefore, a mixture of linkers of different lengths had to be used.

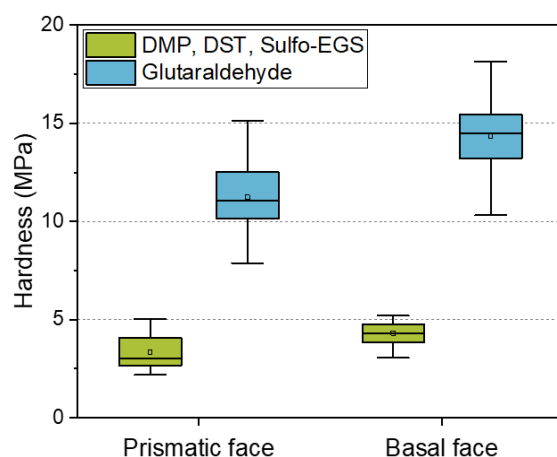


Figure 4. Comparison of the hardness of wild-type crystals cross-linked using the different linkers for 24 h. Results of WT HheG, cross-linked with glutaraldehyde, were adapted with permission from ref. [20]. Copyright © 2019, American Chemical Society.

Because glutaraldehyde tends to self-polymerize, the resulting cross-linking bond lengths are unpredictable [36]. In addition, excessive cross-linking can lead to a decrease in enzymatic activity [35]. For controllable and predictable cross-linking treatment, alternative linkers can be applied. However, our results showed that, using the alternative lysine cross-linker, the hardness of the anisotropic crystal faces decreased by about 70% compared to the cross-linking with the glutaraldehyde. Besides the high stability of CLECs cross-linked with GA, its low price is of great advantage. A kilogram of 50% glutaraldehyde solution costs only about EUR 70. In comparison, alternative linkers cost a thousand times more (DMP: 159 EUR/1 g; DST: 254 EUR/50 mg; Sulfo-EGS: 185 EUR/50 mg). Predicting the mechanical behavior based on a model can therefore bring advantages in terms of financial expenditure and experimental effort. Table 3 summarizes the modeled direction-dependent crystal strength of all intermolecular bonds smaller than 10 Å (cross-linking with GA), or Lys–Lys* bonds with a well-defined distance for alternative cross-linker (6, 9, and 16 Å, compare with Table 1).

Table 3. Summary of the direction-dependent crystal strength modeled using the anisotropic intermolecular cross-linking bonds. Adapted with permission from ref. [20]. Copyright © 2019, American Chemical Society.

	Arg–Arg	Arg–Lys	Lys–Lys	Lys–Lys*
Z	271.77	142	145.4	174.68
X	231.63	137.81	107.04	133.07
Y + 60°	230.52	140.04	105.47	132.11
Y – 60°	230.49	141.84	107.97	135.75

In Figure 5, a comparison of the experimental and modeled results is shown. The experimental and modeled data were interpreted by comparing the percentage differences between the anisotropic faces. For instance, the difference in the hardness of the basal face to the prismatic face of crystals cross-linked at the same conditions (glutaraldehyde or DMP, DST, Sulfo-EGS-linker mix, referred to as Lys–Lys* in Table 3). These percentage differences are shown as a bar (experiment) in Figure 5. Analogously, the percentage difference in the modeling results, e.g., between the anisotropic crystal faces, is shown as a dot–line plot (model). Since the mechanical properties are presented as a distribution, the lower and upper quartile (25% and 75%, respectively) were added for comparison and shown as error bars.

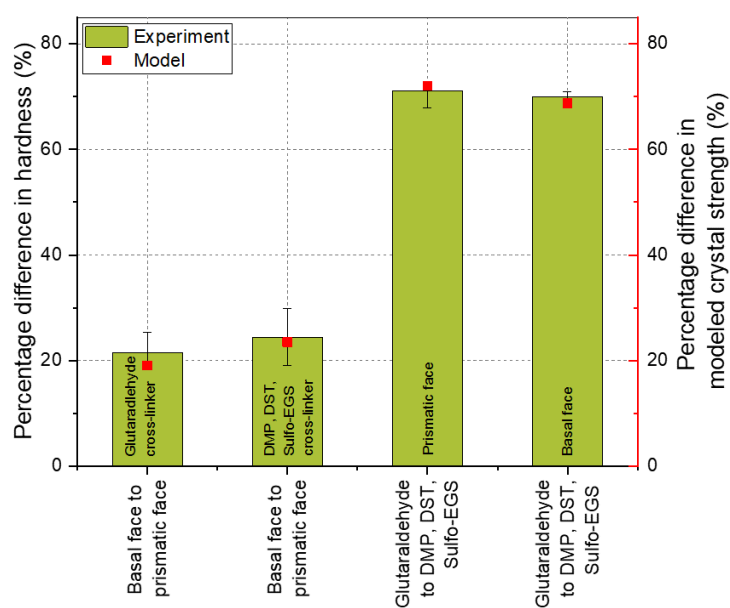


Figure 5. Comparison of the experimental and the modeled results of differently cross-linked wild-type HheG crystals. The bars represent the percentage differences between the mean hardness of the respective crystal faces considered, as described in the diagram. The square dots represent the modeling results, which are also represented as the percentage difference between the corresponding crystal faces. The error bars show the percentage differences of the upper and lower quartiles of the distribution of mechanical properties.

Originally, the model was developed by Kubiak et al. and used to explain the time-dependent anisotropy of wild-type HheG CLECs. The authors showed that crystal strength is direction-dependent due to the cross-linking bonds. The results showed that the crystal strength resulting from the Lys–Lys and Arg–Arg bonds was about 20% higher in the Z-direction (for the basal face), which is consistent with the experimental results. Looking at the cross-linking using the linker mix, it also turns out that the experiment agreed well with the model. The experimentally determined anisotropy between the basal and prismatic faces was about 24%. This corresponded to the difference in crystal strength due to the Lys–Lys bridges from the three defined linker lengths (see Table 3, Lys–Lys*, ratio of bond strength of the Z-direction (174.68) and an average of X, Y + 60°, and Y – 60° (ca. 133.64)). Previously, it was found that the Lys–Lys and Arg–Arg bridges lead to the anisotropic behavior of the HheG crystals. Assuming that there are bonds of all the considered amino acid residue pairs in the crystal, the Arg–Lys bond here did not contribute to the anisotropic behavior of the wild-type HheG crystals, and the bonds in the defined directions were summed up and the total strength of the respective areas for differently cross-linked crystals was proportionally adjusted. The mechanical investigation showed that, due to the use of a linker mix instead of glutaraldehyde, the average hardness of the prismatic and basal crystal faces decreased by about 70%. The results corresponded to the modeling with some slight deviation.

The knowledge that a crystal structure can be used to predict the mechanical behavior of the surfaces saves an enormous amount of time through the targeted selection of the linker and the subsequent model prediction of the crystal strength based on the formed cross-link bridges. The model can be used, for example, to determine which binding-site distances occur most frequently and which crystal strength will correlate with this linker length, and the length of the linker can then be accordingly selected for experimental cross-linking. In addition, it can be determined whether other linkers, e.g., carboxyl or sulfhydryl instead of amine linkers, will provide better mechanical performance. By selectively combining different variants—linker length, type, with binding sites, e.g., far away from the catalytic site—the desired mechanical strength can be modeled in advance.

3.2. Mechanical Properties of Wild-Type HheG Crystals in the Micrometer Range

In the introduction, it was written that protein engineering is a common method for improving the performance of enzymes. Unfortunately, improvements in the properties of solubilized proteins are not always accompanied by improvements in the mechanical stability of the crystals. Figure 6 shows a comparison of the fraction of elastic energy of the wild-type and the D114C crystals mechanically characterized in their native state. From the results, it can be seen that the fraction of elastic energy of the basal face of D114C crystals was significantly lower than that of the wild-type crystals. The difference was about 40% at a 200 nm penetration depth and even almost 60% at a 900 nm penetration depth. In comparison, the difference between prismatic crystal faces was much smaller and lay within the spread of the distribution of mechanical properties.

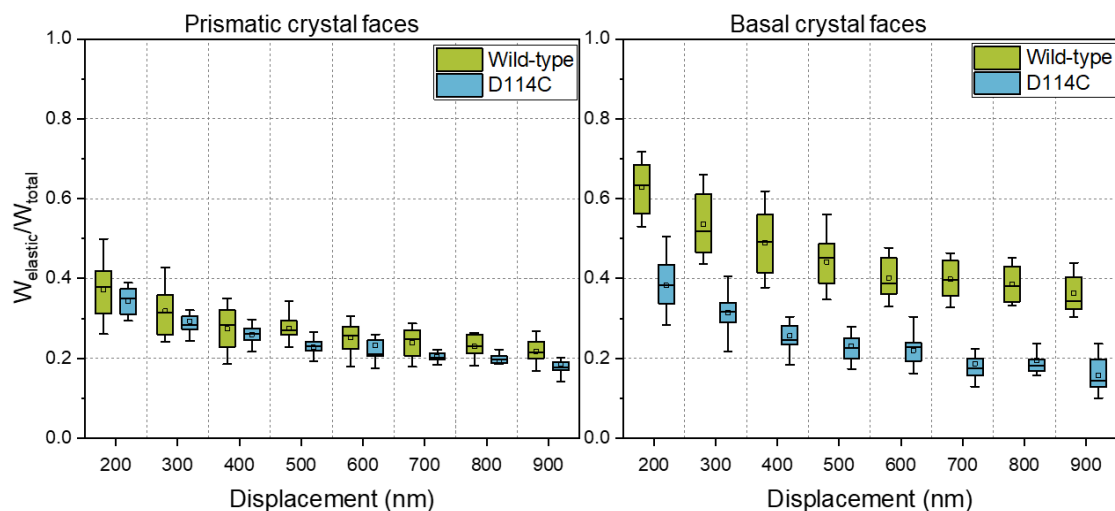


Figure 6. Influence of protein engineering on the fraction of elastic energy of the HheG enzyme crystals.

Most likely, the lowering of the elastic energy fraction of the basal crystal face was due to the point mutation of the crystal contact, which lay exactly along the *c*-axis (*Z*-direction), as shown in Figure 7. Since the crystals were held together in their three-dimensional form by crystal contacts, the mutation of such a site could contribute to the reduction of crystal strength. Kubiak et al. reported that the slip planes are aligned orthogonal to the indenter tip during nanoindentation of the basal crystal face, which is a reason for the easy and unhampered gliding of the planes [22]. For the native D114C crystals, it seems to reduce the interactions between the slip planes such that a lower fraction of elastic energy can be observed.

In a previous study, Kubiak et al. presented and discussed, in detail, the influence of cross-linking on the mechanical behavior of enzyme crystals. The authors also investigated the dominating influence of cross-linking on the mechanical behavior of CLECs [22]. In this section, the influence of the genetic modification of position D114 on the mechanical properties of CLECs is presented. By replacing it with cysteine, a cross-linking site was incorporated, which could be cross-linked by means of a suitable linker—in this case, a BMOE linker—in addition to the lysines. Hence, in the present study, crystals were partially cross-linked using glutaraldehyde and partially using a BMOE linker via the soaking method. In addition, some of the crystal samples were cross-linked first with GA and then with BMOE. All three samples were mechanically examined and compared with the cross-linked wild-type crystals.

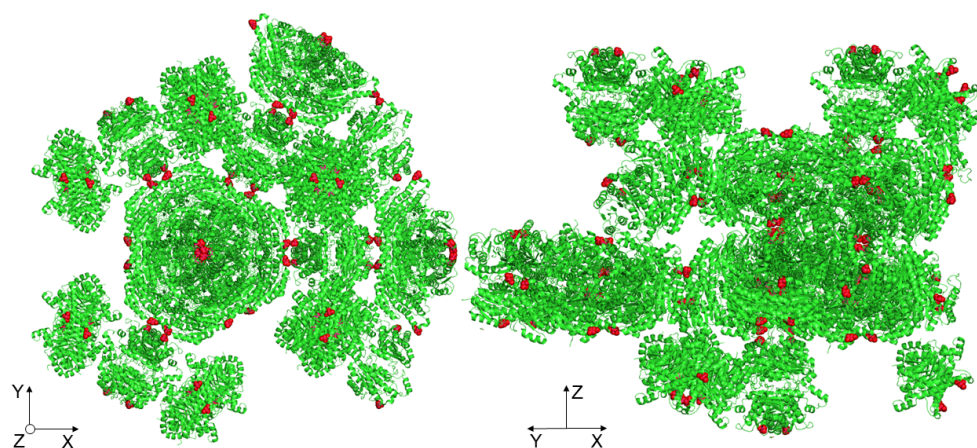


Figure 7. Highlighting the manipulated amino acids (cysteine) at one of the crystal contacts along the *c*-axis (Z-direction).

In Figure 8, the influence of the cross-linker on the elastic energy fraction of the prismatic and basal faces of D114C crystals is presented. From Figure 8, it can be seen that the fraction of elastic energy for both anisotropic faces increased with the degree of cross-linking and was the lowest for cross-linking with the BMOE linker and highest for cross-linking with both linkers. Regarding the prismatic face at the penetration depth of 200 nm, the fractions of elastic energy were 39% (BMOE), 66% (GA), and 69% (GA + BMOE). In comparison, the fraction of elastic energy of the wild-type crystals cross-linked with GA was 64%, which was slightly lower than the median value of D114C crystals that were also cross-linked with GA. Analogous to the results presented earlier about the fractions of elastic energies of native crystals, the fraction of elastic energy decreased with increasing depth. At the penetration depth of 900 nm, the fraction of elastic energy of the crystals cross-linked with BMOE was the lowest at 20% and increased to 40% when the crystals were cross-linked with GA. Due to the double cross-linking (GA + BMOE), the fraction of elastic energy was 7% higher, and at 47%, it was ca. 20% higher than the wild-type crystals. Independent of the cross-linker used, both of the cross-linked crystal faces exhibited a higher fraction of elastic energy than the native crystal faces. It is remarkable for the basal crystal faces that, in contrast to the prismatic faces at the penetration depth of 200 nm, the D114Cs had a lower fraction of elastic energy after cross-linking with GA (64%) than the wild-type crystal (72%). However, the trend was reversed in the deep crystal regions, allowing for the quantification of the stronger influence of cross-linking for the D114C CLECs. For the double cross-linked CLECs, the fraction of elastic energy was the highest and was equal to 51% at a penetration depth of 900 nm. Based on those measurements, it can be concluded that a combination of both strategies—protein engineering and enzyme immobilization—can effectively contribute to the enhancement of mechanical properties of CLECs.

In Section 3.1, the results of hardness measured using AFM at a penetration depth of less than about 30 nm for wild-type crystals were compared with the model. In this section, the model was used for correlation with other mechanical parameters, such as the fraction of elastic energy at a penetration depth of 900 nm. Thus, it was tested whether modeling from a small crystal section was sufficient for the global description of the mechanical behavior. Table 4 shows the results of the direction-dependent crystal strength for the respective pairs of amino acid residues considered for further analysis.

Without cross-linking, plastic deformation is the dominant characteristic deformation behavior of the crystals, whereas with cross-linking, elastic deformation is a decisive factor [22]. For this reason, it was assumed that the cross-linking via additives makes a significant contribution to the elastic stress state within the crystal and, thus, the structure-based modeling approach for the mechanical crystal behavior can be applied to describe the elastic crystal properties with regard to the different crystal directions. In Figure 9,

the results of the nanoindenter are presented, where the anisotropy of the wild-type (WT) crystals was again related to the model based on the differences in the fraction of elastic energy. The fraction of elastic energy of the basal face of the WT CLECs was, on average, about 14% higher than for the prismatic face. Comparing the percentage difference with the summed bond strengths from the bond pairs considered, i.e., Lys–Lys, Lys–Arg, and Arg–Arg, the modeling results also showed a difference of about 14.6% in the Z-direction compared to the X, Y + 60°, and Y – 60° directions ($\sum_{Z\text{-direction}} = 559.17$ and mean of $\sum_{XY\text{-direction}} = 477.59$, cf. Table 3). Thus, based on the modeling results, it can be concluded that all bond pairs contributed to the crystal mechanics in the deep crystal regions. This would also explain why the anisotropy between different crystal faces decreased with increasing penetration depth.

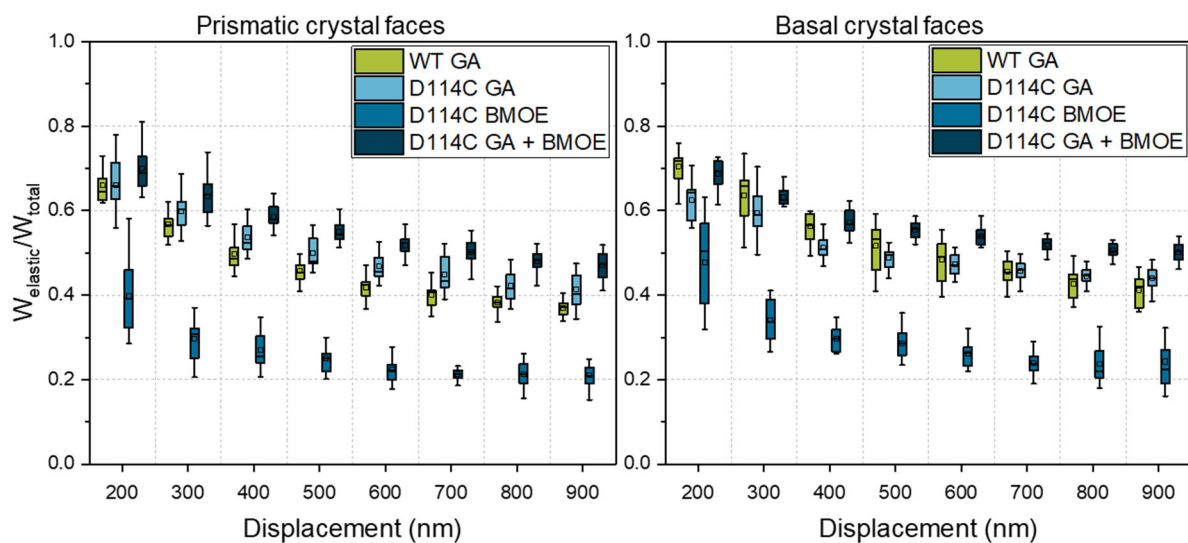


Figure 8. Fraction of elastic energy of prismatic and basal crystal faces of D114C crystals as a function of the cross-linker and penetration depth. To compare the influence of protein engineering on the mechanical behavior of CLECs, wild-type (WT) CLECs, adapted from ref. [22].

Table 4. Summary of the direction-dependent crystal strength of D114C crystals modeled using the anisotropic intermolecular cross-linking bonds.

	Arg–Arg	Arg–Lys	Lys–Lys	Cys–Cys
Z	236.30	217.39	128.73	85.32
X	214.22	236.12	125.99	82.28
Y + 60°	218.54	230.32	128.56	78.66
Y – 60°	216.19	235.65	128.15	78.54

The crystal faces of D114C mutant cross-linked by GA show about a 6% difference in the elastic energy fraction. From Table 4, it can be seen that the sum of Lys–Lys and Arg–Arg bonds (365.03 in the Z-direction and 343.88 in the X, Y + 60°, and Y – 60° directions) also showed about a 6% difference. A similar result concerned the cross-linking using GA and BMOE. Comparable to the cross-linking with GA, the difference between the model and the experimental results was negligible here. The deviation between the model and the result was the highest for cross-linking with BMOE and amounted to 30% when mean values were considered. The reason for this was that the cross-linking of cysteines alone was not sufficient to provide stable support to the crystal lattice such that increased dislocations were observed during the measurement, especially in deeper crystal regions, leading to the increased distribution width of the results. This distribution width could also be seen in the error bars. For example, a positive error bar meant that the percentage difference

of the third quartile (75% of the distribution) of ca. 17% was about 90% higher than the percentage difference of the mean value (9%, see Figure 9). Nevertheless, the model result was within the error or distribution width, which demonstrated the good representation by the experiment. A comparison of the respective crystal faces (basal or prismatic face) between the two crystal structures showed that there was about a 16% deviation of the model from both the third quartile for the prismatic face and from the mean value of the distribution for the basal face.

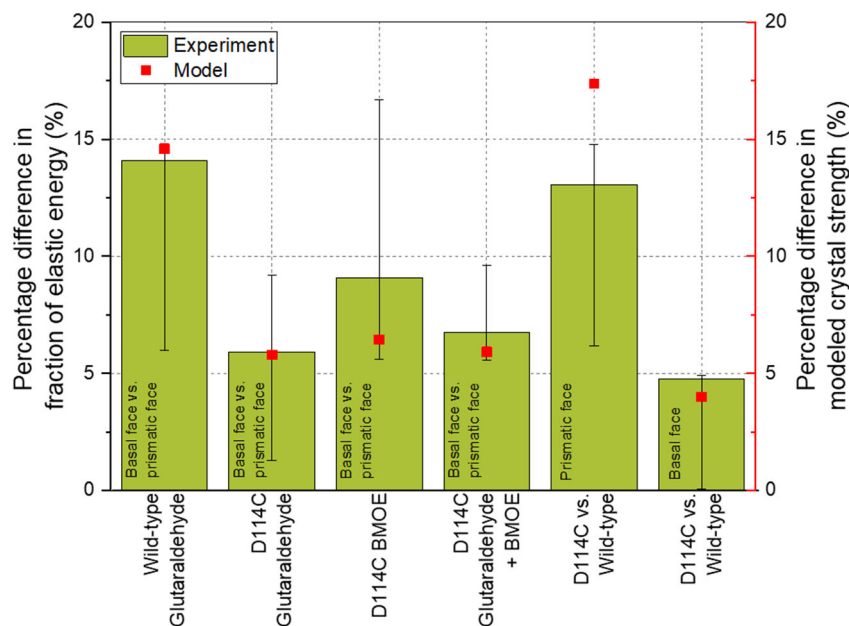


Figure 9. Comparison of the experimental and the modeled results of wild-type HheG crystals and the mutant D114C.

The most important causes, which can have a limiting influence on the modeling of the crystal behavior, can occur at three different stages of experimental execution: X-ray structure analysis, sample preparation, and mechanical measurements. For the model, the X-ray structure analysis was one of the most critical stages. Regarding crystal quality, parameters such as protein production batch or crystallization conditions and growth time may have a great influence. For the mutant D114C, the best-achieved resolution was unfortunately only 3.9 Å, which allowed for the determination of the positions of the atoms with a certain tolerance. During data processing, for example, the symmetry of the respective chains was calculated based on the crystallographic space group. Moreover, the coordinate origin was manually changed. In this process, the atoms were manually shifted to the same origin. However, the coordinates of the atoms were influenced by the B-factors and thus were not rigid but movable in the crystal and did not represent absolute positions but, rather, were relative to each other. The exact displacement measurement of the atoms was limited by the poor resolution, which is why deviations could occur. Due to the relativity of position within a crystal, this was not a critical problem when experiments and modeling were performed using the same crystal structure. However, the error may be significant if different crystal structures are compared to each other. Nevertheless, taking into account the fact that the accuracy of the crystal structures and the developed model were in the angstrom range, the agreement between the model and experiment was surprisingly high for different model proteins.

For the mechanical measurements, influencing factors such as the number of measurement points for a statistically validated estimation of the distribution of mechanical properties and the cantilever quality (geometry or durability of the measurement tip) are important. Using a careful working method, for example, by scanning the crystal surface

to quantify the tilt or by regular SEM images of the cantilevers, these influences can be controlled and, if necessary, minimized.

Another serious factor that influences the modeling of the structure–property relationship is sample preparation. Depending on the formulation parameters, different crystal morphologies can be formed, resulting in differences in mechanical behavior. However, it happened that the mechanical behavior of crystals from different protein batches differed despite the crystal morphology remaining the same. This phenomenon was difficult to explain and was probably due to small differences in ions in the solution after, e.g., the purification or desalting step. Since these influencing factors are difficult to control or avoid despite using established and consistent preparation methods, sample preparation is considered a highly influential factor comparable to that of X-ray structure analysis. Nevertheless, the model reproduced the trends very well. Despite certain limitations, such as the poor resolution of the crystal structure, the model allowed for a reliable representation of the mechanical properties, both the hardness and the elastic part of the deformation energy, within the whole crystal.

The accuracy of this model could be refined by the addition of further information, e.g., regarding the bond strength as a function of bond length. Additionally, X-ray crystallographic studies of cross-linked crystals could also be performed, allowing for the resolution of systematic cross-linking bonds. Subsequently, the relevant distances/positions could be selected and modeled. It would also be possible to introduce a position-dependent strength of interactions instead of cross-linking bridges and, thus, additionally ensure the modeling of the mechanical behavior of non-cross-linked crystals. However, a prerequisite is that accurate quantifiable data on the force fields between individual molecules within the crystal are available, e.g., via molecular dynamics simulation. By combining the data from native and cross-linked crystals, the highest accuracy in terms of predicting the mechanical behavior should be achieved. However, a very high computational capacity is recommended to perform such calculations. The excerpt of crystal structures in this work was limited to 100 Å in space. Despite the relatively small crystal excerpt, the number of rows searched for targeted information in MATLAB was almost 30 million. In order to calculate the data more efficiently, the .pdb file had to be directly converted with suitable functions and limited to relevant information. In case a sensitivity analysis was to be performed using the model, all data must be available. With the help of a high-performance computer, all distances to each other could be calculated and clustered. On a qualitative basis, the amino acid positions could be located, which should be exchanged by the rational protein design to incorporate quite effective cross-linking sites. Assuming that the crystal structure will not be subject to major changes, it should therefore be possible to perform targeted mutations with this tool, which should contribute to enhancing cross-linking and mechanical properties.

4. Summary

The aim of this work was to investigate and elucidate all interactions, limitations, and influences, as well as to establish the guidelines for predicting the mechanical behavior of protein crystals. For this purpose, wild-type and genetically modified model proteins were crystallized, specifically cross-linked, and mechanically examined. Then, a mathematical model was developed, which was based on the respective crystal structure and calculated the distances and their directions between the relevant atoms of the amino acid residues. It then modeled the anisotropic total crystal strength resulting from the potential cross-linking bridges on the basis of a simple function. It was shown that this model could be used to explain all the mechanically studied relationships, such as the anisotropic crystal behavior and the influence of linkers or mutations on the micromechanical properties. By modeling the cross-linking bridges, it was possible to predict which linker length should be used to achieve the desired micromechanical properties or which amino acids should be genetically modified to incorporate positions for particularly effective cross-linking sites. It was also shown that the model could represent cross-linking behavior, as well as cross-

linking tendencies resulting from protein engineering, and thus support the production of tailor-made CLECs.

Author Contributions: Conceptualization, M.K. and C.S.; Data curation, M.K.; Funding acquisition, C.S.; Investigation, M.K.; Methodology, M.K.; Software, M.K. Project administration, I.K. and C.S.; Supervision, I.K. and C.S.; Writing—original draft, M.K.; Writing—review and editing, I.K. and C.S. All authors read and agreed to the published version of the manuscript.

Funding: This work was funded by the German Research Foundation (DFG) within the priority Programme DiSPBiotech (SPP 1934, SCHI 1265/3-2).

Institutional Review Board Statement: Not applicable.

Informed Consent Statement: Not applicable.

Data Availability Statement: The data presented in this study are available within the article.

Acknowledgments: We thank Anett Schallmey and Marcel Staar (Institute for Biochemistry, TU Braunschweig) for the production and purification of the halohydrin dehalogenase proteins and Wulf Blankenfeldt and Steffi Henke for the resolution of the crystal structure of the HheG D114C crystals. We acknowledge financial support from the German Research Foundation and the Open Access Publication Funds of the Technische Universität Braunschweig.

Conflicts of Interest: The authors declare no conflict of interest.

References

1. Schmid, A.; Dordick, J.S.; Hauer, B.; Kiener, A.; Wubbolts, M.; Witholt, B. Industrial biocatalysis today and tomorrow. *Nature* **2001**, *409*, 258–268. [[CrossRef](#)] [[PubMed](#)]
2. Qu, G.; Li, A.; Acevedo-Rocha, C.G.; Sun, Z.; Reetz, M.T. The Crucial Role of Methodology Development in Directed Evolution of Selective Enzymes. *Angew. Chem. Int. Ed. Engl.* **2020**, *59*, 13204–13231. [[CrossRef](#)] [[PubMed](#)]
3. Singh, R.K.; Tiwari, M.K.; Singh, R.; Lee, J.-K. From protein engineering to immobilization: Promising strategies for the upgrade of industrial enzymes. *Int. J. Mol. Sci.* **2013**, *14*, 1232–1277. [[CrossRef](#)] [[PubMed](#)]
4. Truppo, M.D. Biocatalysis in the Pharmaceutical Industry: The Need for Speed. *ACS Med. Chem. Lett.* **2017**, *8*, 476–480. [[CrossRef](#)]
5. Bommarius, A.S.; Riebel, B.R. *Biocatalysis: Fundamentals and Applications*; Wiley-VCH: Weinheim, Germany, 2004; ISBN 3-527-30344-8.
6. Grand View Research. *Market Analysis Report: Enzymes Market Size, Share & Trends Analysis Report by Application (Industrial Enzymes, Specialty Enzymes), by Product (Carbohydrase, Proteases, Lipases), by Source, by Region, and Segment Forecasts 2020–2027*; Grand View Research: Rockville, MD, USA, 2020; pp. 1–173.
7. Buchholz, K.; Kasche, V.; Bornscheuer, U.T. *Biocatalysts and Enzyme Technology*, 2nd ed.; Wiley-Blackwell: Weinheim, Germany, 2012; ISBN 978-3527329892.
8. Brange, J.; Langkjsgmaeligr, L.; Havelund, S.; Vølund, A. Chemical stability of insulin. 1. Hydrolytic degradation during storage of pharmaceutical preparations. *Pharm. Res.* **1992**, *9*, 715–726. [[CrossRef](#)]
9. Sheldon, R.A.; van Pelt, S. Enzyme immobilisation in biocatalysis: Why, what and how. *Chem. Soc. Rev.* **2013**, *42*, 6223–6235. [[CrossRef](#)]
10. Jaeger, K.-E.; Liese, A.; Syldatk, C. *Einführung in die Enzymtechnologie*; Springer: Berlin/Heidelberg, Germany, 2018; ISBN 978-3-662-57618-2.
11. Godoy, C.A.; Fernández-Lorente, G.; de las Rivas, B.; Filice, M.; Guisan, J.M.; Palomo, J.M. Medium engineering on modified *Geobacillus thermocatenulatus* lipase to prepare highly active catalysts. *J. Mol. Catal. B Enzym.* **2011**, *70*, 144–148. [[CrossRef](#)]
12. Stepankova, V.; Bidmanova, S.; Koudelakova, T.; Prokop, Z.; Chaloupkova, R.; Damborsky, J. Strategies for Stabilization of Enzymes in Organic Solvents. *ACS Catal.* **2013**, *3*, 2823–2836. [[CrossRef](#)]
13. Jahangiri, E.; Agharafeie, R.; Kaiser, H.-J.; Tahmasbi, Y.; Legge, R.L.; Haghbeen, K. Medium engineering to enhance mushroom tyrosinase stability. *Biochem. Eng. J.* **2012**, *60*, 99–105. [[CrossRef](#)]
14. Katchalski-Katzir, E. Immobilized enzymes—learning from past successes and failures. *Trends Biotechnol.* **1993**, *11*, 471–478. [[CrossRef](#)]
15. Ansoerge-Schumacher, M.B. Enzymimmobilisierung. In *Einführung in die Enzymtechnologie*; Jaeger, K.-E., Liese, A., Syldatk, C., Eds.; Springer: Berlin/Heidelberg, Germany, 2018; pp. 187–206. ISBN 978-3-662-57619-9.
16. Bernal, C.; Rodríguez, K.; Martínez, R. Integrating enzyme immobilization and protein engineering: An alternative path for the development of novel and improved industrial biocatalysts. *Biotechnol. Adv.* **2018**, *36*, 1470–1480. [[CrossRef](#)]
17. Staar, M.; Henke, S.; Blankenfeldt, W.; Schallmey, A. Biocatalytically active and stable cross-linked enzyme crystals of halohydrin dehalogenase HheG by protein engineering. *ChemCatChem* **2022**, e202200145. [[CrossRef](#)]
18. Navia, M.A.; Clair, N.; Griffith, J.P. Crosslinked enzyme crystals (CLECs™) as immobilized enzyme particles. *Stud. Org. Chem.* **1993**, *47*, 63–73. [[CrossRef](#)]

19. Schallmey, A. Bioinformatische Methoden zur Enzymidentifizierung. In *Einführung in die Enzymtechnologie*; Jaeger, K.-E., Liese, A., Syldatk, C., Eds.; Springer: Berlin/Heidelberg, Germany, 2018; pp. 125–140. ISBN 978-3-662-57619-9.
20. Kubiak, M.; Storm, K.-F.; Kampen, I.; Schilde, C. Relationship between Cross-Linking Reaction Time and Anisotropic Mechanical Behavior of Enzyme Crystals. *Cryst. Growth Des.* **2019**, *19*, 4453–4464. [[CrossRef](#)]
21. Kubiak, M.; Solarczek, J.; Kampen, I.; Schallmey, A.; Kwade, A.; Schilde, C. Micromechanics of Anisotropic Cross-Linked Enzyme Crystals. *Cryst. Growth Des.* **2018**, *18*, 5885–5895. [[CrossRef](#)]
22. Kubiak, M.; Staar, M.; Kampen, I.; Schallmey, A.; Schilde, C. The Depth-Dependent Mechanical Behavior of Anisotropic Native and Cross-Linked HheG Enzyme Crystals. *Crystals* **2021**, *11*, 718. [[CrossRef](#)]
23. Kubiak, M.; Mayer, J.; Kampen, I.; Schilde, C.; Biedendieck, R. Structure-Properties Correlation of Cross-Linked Penicillin G Acylase Crystals. *Crystals* **2021**, *11*, 451. [[CrossRef](#)]
24. Wine, Y.; Cohen-Hadar, N.; Freeman, A.; Frolow, F. Elucidation of the mechanism and end products of glutaraldehyde crosslinking reaction by X-ray structure analysis. *Biotechnol. Bioeng.* **2007**, *98*, 711–718. [[CrossRef](#)]
25. Yonath, A.; Sielecki, A.; Moulton, J.; Podjarny, A.; Traub, W. Crystallographic studies of protein denaturation and renaturation. 1. Effects of denaturants on volume and X-ray pattern of cross-linked triclinic lysozyme crystals. *Biochemistry* **1977**, *16*, 1413–1417. [[CrossRef](#)]
26. Salem, M.; Manguen, Y.; Prangé, T. Revisiting glutaraldehyde cross-linking: The case of the Arg-Lys intermolecular doublet. *Acta Crystallogr. Sect. F Struct. Biol. Commun.* **2010**, *66*, 225–228. [[CrossRef](#)]
27. Buch, M.; Wine, Y.; Dror, Y.; Rosenheck, S.; Lebendiker, M.; Giordano, R.; Leal, R.M.F.; Popov, A.N.; Freeman, A.; Frolow, F. Protein products obtained by site-preferred partial crosslinking in protein crystals and “liberated” by redissolution. *Biotechnol. Bioeng.* **2014**, *111*, 1296–1303. [[CrossRef](#)]
28. Rumpf, H.C.H. Zur Theorie der Zugfestigkeit von Agglomeraten bei Kraftübertragung an Kontaktpunkten. *Chem. Ing. Tech.* **1970**, *42*, 538–540. [[CrossRef](#)]
29. Schilde, C.; Burmeister, C.F.; Kwade, A. Measurement and simulation of micromechanical properties of nanostructured aggregates via nanoindentation and DEM-simulation. *Powder Technol.* **2014**, *259*, 1–13. [[CrossRef](#)]
30. Schilde, C.; Westphal, B.; Kwade, A. Effect of the primary particle morphology on the micromechanical properties of nanostructured alumina agglomerates. *J. Nanopart. Res.* **2012**, *14*, 2344. [[CrossRef](#)]
31. Schilde, C.; Kwade, A. Measurement of the micromechanical properties of nanostructured aggregates via nanoindentation. *J. Mater. Res.* **2012**, *27*, 672–684. [[CrossRef](#)]
32. Jegan Roy, J.; Emilia Abraham, T. Strategies in making cross-linked enzyme crystals. *Chem. Rev.* **2004**, *104*, 3705–3722. [[CrossRef](#)]
33. Barbosa, O.; Ortiz, C.; Berenguer-Murcia, Á.; Torres, R.; Rodrigues, R.C.; Fernandez-Lafuente, R. Glutaraldehyde in bio-catalysts design: A useful crosslinker and a versatile tool in enzyme immobilization. *RSC Adv.* **2014**, *4*, 1583–1600. [[CrossRef](#)]
34. Yan, E.-K.; Cao, H.-L.; Zhang, C.-Y.; Lu, Q.-Q.; Ye, Y.-J.; He, J.; Huang, L.-J.; Yin, D.-C. Cross-linked protein crystals by glutaraldehyde and their applications. *RSC Adv.* **2015**, *5*, 26163–26174. [[CrossRef](#)]
35. Margolin, A.L. Novel crystalline catalysts. *Trends Biotechnol.* **1996**, *14*, 223–230. [[CrossRef](#)]
36. Whipple, E.B.; Ruta, M. Structure of aqueous glutaraldehyde. *J. Org. Chem.* **1974**, *39*, 1666–1668. [[CrossRef](#)]